Electronic Supplementary Material (ESI) for Nanoscale.

SUPPORTING INFORMATION

Aggregation of Polyethylene glycol Polymers Suppresses Receptor-mediated Endocytosis of PEGylated Liposomes

Zhiqiang Shen

Department of Mechanical Engineering, University of Connecticut, Storrs, CT 06269, USA.

Huilin Ye

Department of Mechanical Engineering, University of Connecticut, Storrs, CT 06269, USA.

Martin Kröger

Department of Materials, Polymer Physics, ETH Zurich, CH-8093 Zurich, Switzerland

Ying Li

Department of Mechanical Engineering and Institute of Materials Science, University of Connecticut, Storrs, CT 06269, USA.

E-mail: yingli@engr.uconn.edu

1. Computational Model and Methodology

1.1. DPD Method

All simulations performed in the course of this study are based on the DPD method, a coarse-grained molecular dynamics simulation technique. DPD simulations can correctly and accurately capture hydrodynamics of complex fluids, while retaining essential information about the structural properties of the system components [1, 2]. The DPD method has been widely used and successfully applied for studying problems related to behaviors of lipid vesicles or polymers and their interactions with lipid bilayers. [3–12] The basic interacting sites in DPD simulations are represented by soft beads. Between each pair of DPD beads, effective two-body interactions consist of three major forces [1, 2]: a conservative force $\mathbf{F}^C$, a random force $\mathbf{F}^R$ and a dissipative force $\mathbf{F}^D$. Specifically, the conservative force between beads i and j is $\mathbf{F}_{ij}^C = a_{ij}\omega(r_{ij})\mathbf{e}_{ij}$, where r_{ij} denotes the distance between the two beads i and j, and $\mathbf{e}_{ij}$ is the unit vector pointing from i to j; a_{ij} represents the maximum repulsion force. The weighting factor $\omega(r_{ij})$ is a normalized distribution function as $\omega(r_{ij}) = 1 - r_{ij}/r_0$ for $r_{ij} \leq r_0$, while $\omega(r_{ij}) = 0$ for $r_{ij} > r_0$. Here r_0 is the cutoff distance for pairwise interactions. The random forces are specified by $\mathbf{F}_{ij}^R = \sqrt{2\beta_{ij}k_{\mathrm{B}}T/\Delta t}\,\omega(r_{ij})\alpha\mathbf{e}_{ij}$, where α represents a normal distributed Gaussian random number with zero mean and unit variance, Δt denotes the integration time step, β_{ij} is a bead friction coefficient taken as below [13, 14]:

$$\beta_{ij} = \begin{cases} 4.5 & a_{ij} < 35 \\ 9.0 & 35 \leq a_{ij} < 75 \\ 20.0 & a_{ij} \geq 75 \end{cases} \tag{1}$$

k_{B} and T stand for Boltzmann's constant and temperature, respectively. The dissipative force is given by $\mathbf{F}_{ij}^D = -\beta_{ij}\omega^2(r_{ij})(\mathbf{e}_{ij} \cdot \mathbf{v}_{ij})\mathbf{e}_{ij}$, where $\mathbf{v}_{ij}$ is the relative velocity vector between beads i and j. The conservative force is a purely repulsive interaction, while the random and dissipative forces acting along the centers of the soft beads conserve linear and angular momentum, respectively.

1.2. Lipid and PEG Models

All the lipid molecules in our simulations share the same model, in which two lipid tails (with four tail beads each) are connected with two head beads respectively. And the head group contains three head beads. Adjacent beads making the lipid molecules are connected by the harmonic spring potential $U_{s1} = K_{s1}(r_{ij} - r_{s1})^2$, with spring coefficient $K_{s1} = 64$ $k_{\mathrm{B}}T/r_0^2$, and equilibrium distance $r_{s1} = 0.5r_0$. The stiffness of the lipid tails is guaranteed by an angular potential $U_{\theta 1} = K_{\theta 1}(1 - \cos\theta)$ with $K_{\theta 1} = 15k_{\mathrm{B}}T$. Pair-wise interactions a_{ij} between lipid beads are listed in Table S1. Under control of these parameters, the tension of planar bilayer follows a linear relation with the lipid molecular area [14, 15]. The surface tension of planar bilayer is defined as the integral of difference between normal and lateral component of the pressure tensor [16, 17]:

$$\begin{aligned}\Sigma &= \int dz[p_{zz}(z) - 1/2(p_{xx}(z) + p_{yy}(z))] \\ &= A^{-1}\sum_{i<j}(F_{ij,z}z_{ij} - 1/2(F_{ij,y}y_{ij} + F_{ij,x}x_{ij}))\end{aligned} \tag{2}$$

where z-axis is the normal direction of the planar bilayer interface. p_{zz}, p_{yy} and p_{xx} are the pressure components along the z, y and x directions, respectively. A is the area of the xy-plane. F_{ij} is the conservative force between particles i and j. The stretch modulus of membrane can be obtained by the slope in Fig. S1, $K_A = 17.42k_{\mathrm{B}}T/r_0^2$. And the bending rigidity of membrane obtained from $\kappa = K_A d_{\mathrm{HH}}^2/48$ [18, 19] is round $\kappa \approx 6\ k_{\mathrm{B}}T$.

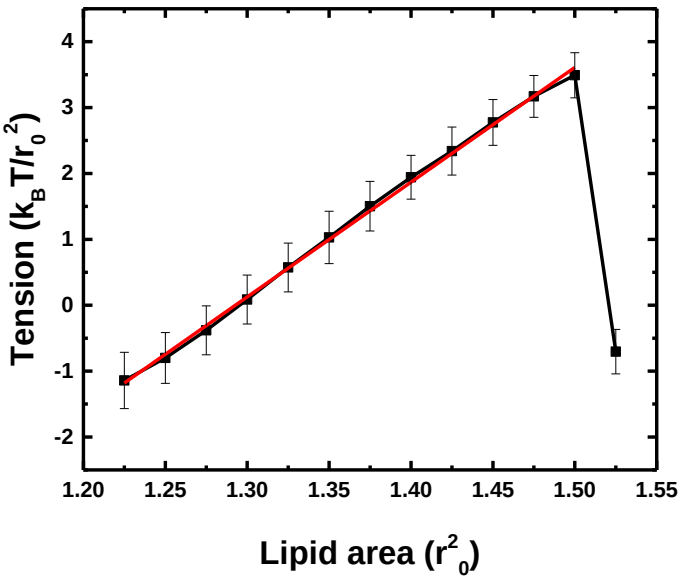

Figure S1: Relation between membrane tension and lipid area.

A hydrophilic PEG polymer in DPD simulations is modeled by a linear chain consisting of coarse-grained monomers. The monomers of PEG polymers are sequentially connected by a harmonic bond potential: $U_{s2} = K_{s2}(r_{ij} - r_{s2})^2$, with spring stiffness $K_{s2} = 2111.3k_{\mathrm{B}}T/r_0^2$ and equilibrium distance $r_{s2} = 0.4125r_0$. The flexibility of the PEG polymer is tuned by an angular potential between each three consecutive monomers, defined by $U_{\theta 2} = K_{\theta 2}(\cos\theta - \cos\theta_0)^2$, with bending stiffness $K_{\theta 2} = 16.4946k_{\mathrm{B}}T$, and equilibrium angle $\theta_0 = 130°$. Such a DPD PEG model could correctly reproduce the conformation of a PEG polymer in water, including the radius of gyration and end-to-end distance, as shown in our previous studies [10, 20]. To describe the PEGylated lipid, one end of the PEG polymer is bonded to the lipid head through a harmonic bond potential. And the monomer on the free end of a PEG polymer is considered as targeting moiety. The molecular weight of a PEG polymer in experiments ranges from 500-5000 Da [21–23]. Note that tethered PEG polymers with large molecular weight on surface leads to a pronounce growth in NP size, which requires

tremendous computational cost to finish the membrane wrapping process. The polymerization degree N of PEG polymers in our simulation is set as $N = 30$ (representing a molecular weight around 1000 Da), to reach a balance between computational efficiency and generality.

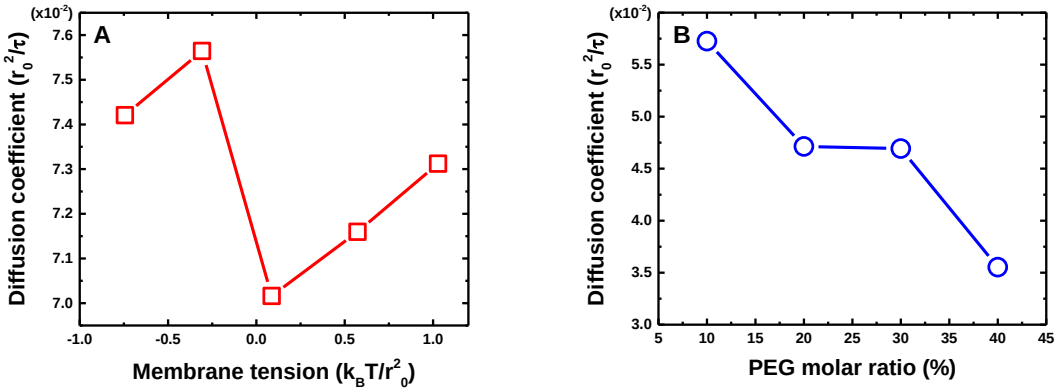

Figure S2: Diffusion coefficient of receptors in planar membrane and ligands on liposome surface. (A) Diffusion coefficients of receptors in planar membrane under different membrane tensions. (B) Diffusion coefficients of receptors on liposome surface with different PEG molar ratios. The radius of liposome is $R = 7r_0$.

To explore the influence of membrane tension on the diffusion of receptor, we calculate its diffusion coefficients under different membrane tensions. The diffusion coefficient of receptor in the planar membrane is obtained from measuring mean squared displacement, $D_{\text{lipid}} =< (\Delta x)^2 + (\Delta y)^2 > /4t$, where Δx and Δy are the displacements of receptors in planar directions x and y respectively. t is the time difference over which diffusion is tested. As shown in Fig. S2.A, the receptor diffusion coefficients only slightly change with membrane tensions. The deviation of diffusion coefficients is less than 9%, which indicates that the diffusion of receptors in membrane is irrelevant to the membrane tension, which is consistent with experimental results [24]. Moreover, we calculate the receptor diffusion coefficient $D_{\text{lipid}} \simeq 7.3 \times 10^{-2}\, r_0^2/\tau$ by averaging the values under different tensions.

The diffusion of ligand on the free end of PEG polymers might be affected by the variation of PEG polymer molar ratio on the liposome surface. We then further tested the ligand diffusion coefficients. The ligands on PEG polymers are directly connected with the PEGylated lipids in liposome. Here, we measured the diffusion coefficients of PEGylated lipids to reflect the diffusion behaviors of ligands. The lateral diffusion coefficient of PEGylated lipid is calculated from its mean squared displacement on the spherical liposome surface. Therefore, the diffusion coefficient of ligand is given by [25] $D_{\text{ligand}} =< 4R^2\varphi^2 > /t$, where R is the radius of liposome. φ is the angle between the membrane normal vector at $t = 0$ and $t = t$. The normal vector is defined as the connecting vector between center-of-mass (COM) of liposome and COM of the PEGylated lipid. Here, the diffusion coefficient is obtained by fitting the mean squared displacement in the first 10^6 time steps. As given in Fig. S2.B, due to the tightly packing between PEG polymers under higher moral ratio, the diffusion coefficient of ligand D_{ligand} decreases with the increasing of PEG molar ratio. More

important, the diffusion coefficient of ligand D_{ligand} is smaller than that of receptor.

Within our DPD model, different types of beads have identical masses and cutoff distances for pairwise interactions. For the sake of transferability, the mass, length and time scales are all normalized. The unit length is taken to be the cutoff distance r_0. The unit mass is m for all the beads and is set to unity. In addition, the unit energy is defined by the thermal energy $k_{\text{B}}T$. All other dimensional quantities can thus be uniquely made dimensionless in terms of these basic units (and vice versa).

The time step in our DPD simulations is chosen as $\Delta t = 0.01\tau$, with $\tau = \sqrt{mr_0^2/k_{\text{B}}T}$. The number density of beads in the simulation box is fixed at $3/r_0^3$ [2]. The velocity-Verlet integration algorithm is adopted for the time integration. The reduced units can be mapped to SI units using a real bilayer thickness and a measured value for the in-plane diffusion coefficient of lipids, as shown in previous studies [14,15]. From the experiments, the thickness of membrane is $d_{\text{HH}} \approx 3.53$ nm [26] and thickness in our simulation is $d_{\text{HH}} \approx 4\ r_0$. The physical length scale could then obtained by the relation of $r_0 \simeq 0.9$ nm. Comparing the experimental lipid lateral diffusion coefficient $D \simeq 5\ \mu\text{m}^2/s$ of DMPC [27] and one in our simulation $D_{\text{lipid}} \simeq 7.3 \times 10^{-2}\ r_0^2/\tau$, we can obtain the physical time scale $\tau = 11.8$ ns. Periodic boundary conditions are applied along all directions of the simulation box. All the simulations are performed by using the Large-scale Atomic/Molecular Massively Parallel Simulator (LAMMPS), distributed by Sandia National Laboratories [28].

Table S1: Interaction parameters, a_{ij}, between beads i and j, in the DPD simulation. S, H, T, and E represent solvent (water), lipid head, lipid tail, and PEG beads, respectively.

a_{ij} $[k_{\text{B}}T/r_0]$	S	H	T	E
S	25.0	30.0	75.0	26.3
H	30.0	30.0	35.0	26.3
T	75.0	35.0	10.0	33.7
E	26.3	26.3	33.7	25.0

1.3. Simulation Protocol

To prepare the PEGylated NPs, lipid molecules is firstly randomly distributed into a simulation box to form a liposome through self-assembly process at temperature $T = 1.0$. Then certain number of lipids in the outer layer is randomly chosen to graft with PEG chains on the lipid head beads according to the targeted PEGylated lipid molar ratio. The PEGylated liposomes then further relax for $1 \times 10^6\ \tau$ under temperature of $T = 1.0$. Two kinds of liposomes with 800 and 1701 lipids are prepared. Their radius sizes are around 7 r_0 and 15 r_0, respectively. Planar membrane bilayer is relaxed in the box size of $(70 \times 70 \times 100)\, r_0^3$, which is large enough to avoid the influence of simulation box size on endocytosis. Finally, the fully relaxed PEGylated liposomes are placed above the planar bilayer to investigate the membrane wrapping process. During this process, to explore the effect of PEG mobility,

bilayer in liposome and the included water beads are treated with three different ways: (1) No additional restriction is applied on the liposome, such that the liposome itself is able to deform under stress and the PEGylated lipid could freely diffuse on the surface because of the fluid state of the bilayer; (2) All of the lipid molecules and the water beads inside together are considered as a single rigid body, which means that the liposome could not deform (like a solid NPs) and the tethered points of PEG polymers are fixed on the surface; (3) All the water beads inside liposome are treated as a single rigid body, in which situation the liposome can hardly deform under stress because of the rigid water core, while the PEG polymer can still move on the liposome surface. Following these procedures, we can ensure that the chemical properties of all the PEGylated NPs are the same. By comparing the differences during endocytosis of these three kinds of NPs, we can clearly reveal the influence of PEG mobility on endocytosis.

During endocytosis, in view of the length scale difference between the NP (< 100 nm) and cell (~ 10 μm), the internalization of NPs should not affect the surface tension of the cell membrane. To mimic this condition and reproduce the constant membrane surface tension in our DPD simulations, we adopt the N-varied DPD method. Instead of controlling the lateral pressure/force of the membrane, this method takes an alternative approach to ensure a constant membrane tension, by controlling the number of lipids per unit area. It has been widely used to study the endocytosis of NPs in DPD simulations [10, 20, 29–31]. In practice, the boundaries of the lipid bilayer are treated as a lipid reservoir for the addition and removal of lipids. If the lipid number per unit area is larger (or smaller) than the target density ρ_1 (or ρ_2), lipid molecules will be deleted (or inserted) into this boundary region to maintain a constant lipid number density. Meanwhile, a corresponding number of water molecules will be inserted (or deleted) randomly in the simulation box to ensure a constant water bead density of $3.0/r_0^3$ in the DPD simulations. By using the N-varied DPD protocol, the lipid density in the membrane is easily controlled to maintain the membrane's lateral tension during the endocytosis process.

To mimic the ligand-receptor interaction, we assume that 50% of the lipid molecules in the planar bilayer act as receptors, which means that the number of receptors is large enough compared to the number of ligands on the NPs surface. Then, the receptor diffusion induced limited efficiency [32] in the endocytosis could be excluded in our simulations. The targeting moieties (ligands) conjugated to the free ends of PEG polymers interact with receptors as following:

$$U_{ij} = \begin{cases} 4\epsilon_{\text{ligand}}[(\sigma_b/r_{ij})^{12} - (\sigma_b/r_{ij})^6] - U_{\text{cut}}, & r_{ij} <= r_{\text{cut}} \\ 0, & r_{ij} > r_{\text{cut}} \end{cases} \tag{3}$$

Here, $r_{\text{cut}} = r_0$ for a short-range attractive interaction. $U_{\text{cut}} = 4\epsilon_{\text{ligand}}[(\sigma_b/r_0)^{12} - (\sigma_b/r_0)^6]$. The equilibrium distance is fixed to be $\sigma = 0.624 r_0$. Additionally, the repulsive force is set to be 25 $k_{\text{B}}T/r_0$, if it is larger than 25 $k_{\text{B}}T/r_0$. Then the ligand-receptor binding strength could be computed as:

$$\epsilon_b = \ln\{1 + \int_0^\infty dr[\exp(-U_{ij}) - 1]\} \tag{4}$$

Here we set $\epsilon_{\text{ligand}} = 12 k_{\text{B}}T$, corresponding to the binding strength around $6.8 k_{\text{B}}T$.

1.4. Self-consistent mean field theory

To interpret the DPD simulation results and reveal the underlying physical mechanism, we employ an independent self-consistent field (SCF) theoretical approach to estimate the free energy of PEG polymers with fixed tethered point. The SCF result allows us to calculate the radial volume fraction profile $\phi(r)$ of the spherical brush, the volume fraction profile of the terminal monomers, $\phi(r)$ and the corresponding free energy, F_{polymer}. The measured PEG profiles could be recovered using a simplest classical model of a polymer under good solvent conditions [10, 20], which is characterized by a dimensionless mixing free energy density $\nu f_m(\phi) = \tau\phi^2 + \omega\phi^3$ with $\tau = \omega = 1$, where $\nu = 0.0633$ nm^3 denotes the excluded volume of a PEG monomer. Within the SCF we basically aim at minimizing a single chain free energy function that is composed of elastic and interaction parts,

$$\frac{F_p}{k_{\mathrm{B}}T} = \frac{3}{2}\frac{\langle r_{\mathrm{ee}}^2\rangle}{R_0^2} + \int f_m(\phi)d^3r \tag{5}$$

where $\langle r_{\mathrm{ee}}^2\rangle = V^{-1}\int(r - d/2)^2\phi d^3r$ is the mean squared extension of a polymer that is tethered on a sphere of diameter d, properly normalized by the occupied chain volume $V = \int \phi d^3r = N\nu$, and $R_0 = R_0(N)$ represents the equilibrium size of a PEG polymer. Here we take $R_0^2 = \langle R_{\mathrm{ee}}^2\rangle/e$, using the available $R_{\mathrm{ee}}^2(N)$ values for a single PEG chain. The above free energy is minimized with respect to the volume fraction profile, subject to the constraint of conserved V and the tethering condition, $\phi(r < d/2) = 0$. A most common numerical implementation of the related optimization problem on a geometry-adapted grid have been introduced by Scheutens and Fleer [33]. We follow the implementation described in detail by Wijmans and Zhulina [34]. To this end, a single flexible polymer is grown sequentially, using a constant bond length $a = 0.33\, r_0$ (for PEG), starting from a spherical surface of diameter d. During random growth within the space surrounding the NP, the representative chain creates its own radial volume fraction profile to which it reacts, as the volume fraction enter the probability to choose from all possible directions, at each step of growth procedure. To be precise, it reacts by its current radial coordination r to the dimensionless exchange chemical potential $U(\phi)/k_{\mathrm{B}}T = \nu f_m'(\phi) = 2\phi + 3\phi^2$ contained in a segment weighting factor $G_1(r) = \exp(-U(r)/k_{\mathrm{B}}T)$, where we recall that $\phi = \phi(r)$. The problem is thus closely related to a diffusion process in the presence of a potential and boundary, and can in principle also be formally treated using Green's functions. Accordingly, one introduces $G_n(r)$, the average statistical weight of an n-mer of which the last segment is located in layer r. $G_n(r) = G_{n-1}(r)G_1(r)$ for $n = 2, \ldots, N$, where the spatial average is taken over a sphere of radius a. We are left with a closed set of coupled equations, where the average play the role of the coefficients of a linear system of equations that can be solved in an iterative fashion using simple matrix inversions. Due to head-tail symmetry of the polymer chains, the volume fraction profile of an n-mer is subsequently obtained from the solution $G_n(r)$ via $\phi(r) = C_nG_n(r)G_{N-n+1}(r)/G_1(r)$, where the C_n's are normalization factors that follow from $\nu = \int \phi(r)d^3r$ and finally $\phi(r) = \Sigma_{n=1}^N\phi(r)$ as well as $\phi_N(r)$ are obtained. Because the volume fraction profiles ϕ of the unwrapped PEGylated NP are all well recorded, we

can estimate the free energy difference $\Delta F_{\text{polymer}} = \Delta F_p$ between wrapped and unwrapped PEGylated NP upon inserting the two measured $\phi(r)$'s separately in to Eq.5

1.5. Computation of membrane energy

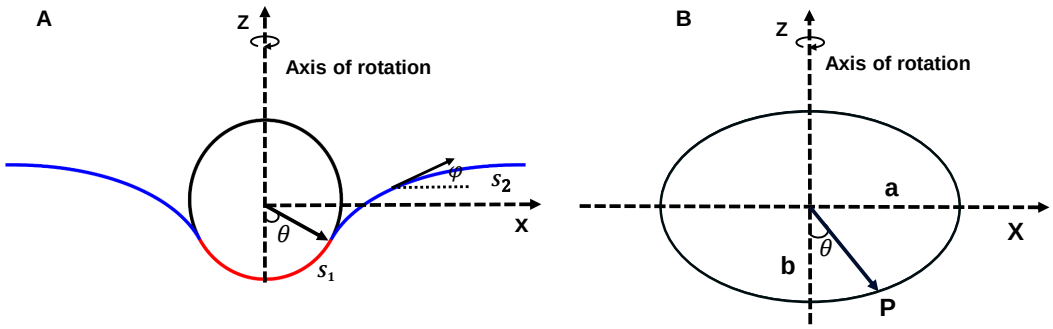

Figure S3: (A) Illustration of membrane wrapping geometry and parameters. θ is the wrapping angle. S is the arc length. ϕ is the angle tangent to the membrane profile. The wrapping region of membrane is represented by red line. The free part of membrane is represented by the blue line. (B) Illustration of an ellipsoidal nanoparticle. a and b are the lengths of half major and minor axes, respectively.

To estimate the membrane elastic energy in our simulations, a theoretical model is developed. In the theory, we assume that a planar membrane wraps around a solid NP (cf. Fig. S3.A), which has rotational symmetry with the axis z. Based on the Canham-helfrich's framework [35], the total elastic energy of membrane under certain wrapping angle could be described as

$$E_{\text{MEM}} = E_{\text{MBend}} + E_{\text{MTen}} \tag{6}$$

where E_{MBend} is the membrane bending energy. E_{MTen} represents the membrane tension energy. In our model, we consider a symmetric membrane and assume no topological change during the whole wrapping process. Then the bending energy for the membrane could be expressed as:

$$E_{\text{MBend}} = \int_S \kappa(c_1 + c_2)^2 ds \tag{7}$$

where, κ is the membrane bending rigidity. c_1 and c_2 are the principle curvatures on the membrane surface, respectively. The tension energy could be calculated by

$$E_{\text{MTen}} = \sigma \Delta S \tag{8}$$

where σ is the membrane tension and ΔS is the excess area caused by the bending of membrane.

1.5.1. Spherical nanoparticle As illustrated in Fig. S3, the elastic energy of membrane could be divided into two parts:(1) the wrapping part and (2) the free part. The geometry of the wrapping part is determined by the shape of NP. For a spherical NP, the bending energy in the wrapping part is $E_{\mathrm{Bwrap}} = 4\pi\kappa(1-\cos\theta)$. And the corresponding tension energy is $E_{\mathrm{Twrap}} = \pi r^2\sigma(1-\cos\theta)^2$, where r is the radius of spherical NPs. To calculate the membrane geometry of the free part, we assume tangent angle $\phi(s_2)$ has a Fourier series from with respect to the free part of arch length s_2 [36, 37].

$$\phi(s_2) = \phi_0 + \frac{\phi_1-\phi_0}{L}s_2 + \sum_{i=1}^{n} a_i \sin\left(\frac{\pi}{L}is_2\right) \tag{9}$$

where a_i is Fourier amplitude and L is the total arch length of free part membrane. ϕ_0 is the tangent angle of membrane in the contact region between wrapping and free parts. ϕ_1 is the tangent angle of membrane far away from NPs. This kind of method has been successfully applied to explore the profile of vesicle induced by the interactive NPs in the works of Gozdz et al. [36] and Wang et al. [37]. To satisfy the boundary condition, in the connecting region, both $\phi_0 = \theta$ and $z(0) = r - \cos(\theta)r$ should be satisfied to ensure the smooth connection between wrapping and free parts of membrane. In the region far wary from NPs, $\phi_1 = 0$ and $\frac{d\phi}{ds_2} = 0$, which can ensure the bending and tension energies vanish for the membrane far wary from NPs [38]. More terms in Fourier series are better, for the free part of membrane here, we find that $n = 20$ could already well describe the profile of deformed membrane. After characterization, the membrane bending and tension energies of free part could be obtained by

$$E_{\mathrm{Bfree}} = \pi\kappa\int_0^L r_s(s_2)[\frac{d\phi}{ds_2} + \frac{\sin\phi}{r_s(s_2)}]^2 ds_2, \tag{10}$$

$$E_{\mathrm{Tfree}} = \sigma\int_0^L \pi r_s(s_2) ds \tag{11}$$

where $r_s(s_2) = \int_0^{s_2}\cos\phi ds' + \sin(\theta)r$. Then the total elastic energy of free part becomes a function of a_i and L. By performing the energy minimization, we could get the profile of membrane and the energy of $E_{\mathrm{Bfree}} + E_{\mathrm{Tfree}}$. We use the particle swarm optimization (PSO) algorithm to do the numerical optimization [39].

1.5.2. Ellipsoidal nanoparticle For an ellipsoidal NP with shape function of $(x^2+y^2)/a^2 + z^2/b^2 = 1$ (a and b are the lengths of half major and minor axes, respectively), the bending energy of the wrapping part could be obtained by $E_{\mathrm{Bwrap}} = 2a^2\pi\kappa\int_0^\theta M(\theta')d\theta'$, where $M(\theta) = \frac{\lambda}{2a}\frac{1+\cos^2\theta+\lambda^2\sin^2\theta}{(\cos^2\theta+\lambda^2\sin^2\theta)^{3/2}}$ is the mean curvature at the point P $= (a\sin\theta, -b\cos\theta)$ on the ellipsoid, $\lambda = b/a$. The tension energy of wrapped part could then be calculated by $E_{\mathrm{Twrap}} = \sigma(S(\theta) - \pi r_s^2(\theta))$, where $S(\theta) = 2a^2\pi\int_0^\theta \sin\theta(\cos^2\theta + \lambda^2\sin^2\theta)d\theta$ is the surface are of the wrapped part. And $r_s(\theta) = a\sin\theta$ is the distance from the point P to the axis of rotation. In addition, the boundary conditions at the connection between wrapping and free parts $\tan(\phi_0) = b/a\tan\theta$ and $z(0) = b - b\cos\theta$ are satisfied. Also, $r_s(s_2)$ in the Eq. 11 follows the relation as $r_s(s_2) = \int_0^{s_2}\cos\phi\, ds' + a\sin\theta$. All other procedures are the same as spherical NP.

2. Endocytosis of large PEGylated rigid nanoparticle

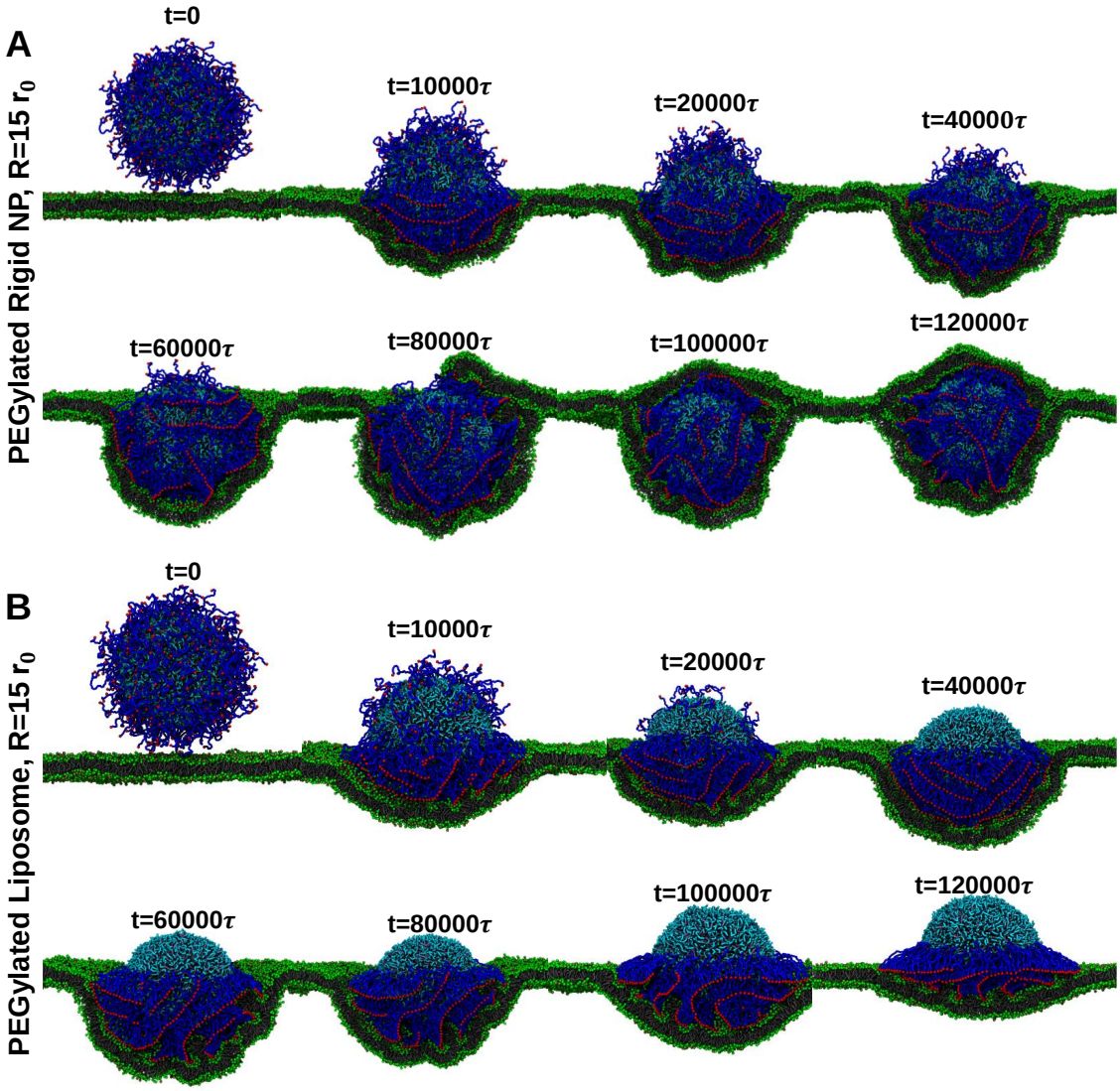

Figure S4: Representative snapshots for membrane wrapping processes of (A) PEGylated rigid NP and (B) PEGylated liposome with size of $r = 15\ r_0$. The membrane tension in both cases is controlled at $0.08\ k_{\mathrm{B}}T/r_0^2$. Water beads are not shown for clarity.

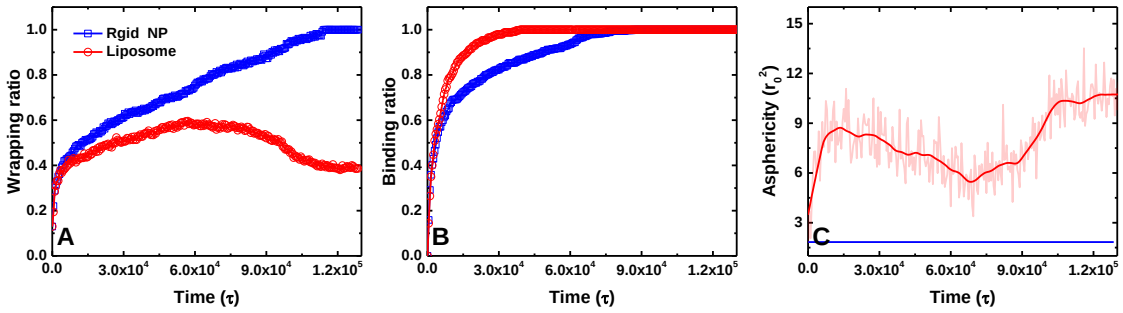

Figure S5: Comparison of (A) wrapping ratio, (B) ligand-receptor binding ratio and (C) asphericity between PEGylated rigid NP and liposome during the membrane wrapping process in Fig.S4.

3. Endocytosis of PEGylated nanoparticle with rigid water core

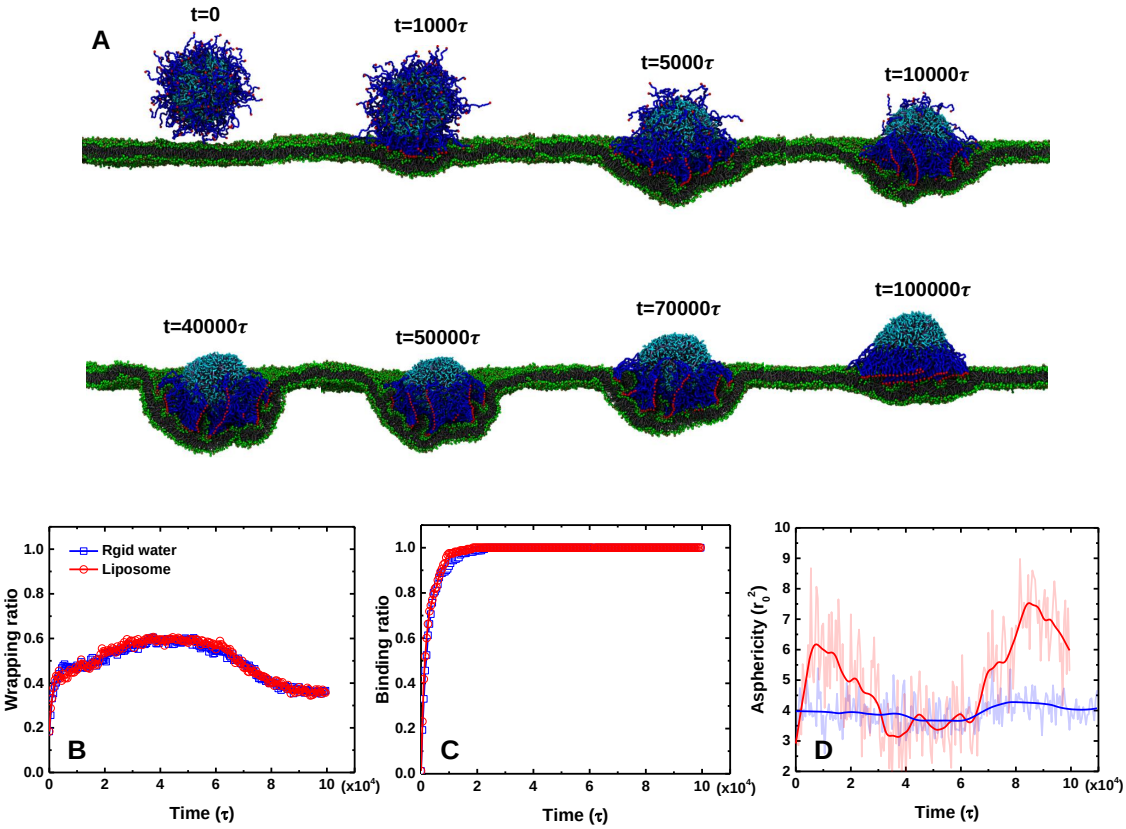

Figure S6: Endocytosis of 20 mol% PEGylated nanoparticle with rigid water core under membrane tension of $-0.038k_{\mathrm{B}}T/r_0^2$. (A) Snapshots of PEGylated nanoparticle with rigid water core during endocytosis. (B-C) Comparison of wrapping ratio, ligand-receptor binding ratio and asphericity between PEGylated rigid water NP here and the PEGylated liposome in Fig. 2 of the main text.

To further exclude the influence from liposome deformation, we try to explore the membrane wrapping of PEGylated nanoparticle with rigid water core. Here, the water beads inside the liposome in the main text of Fig. 2B are treated as a single rigid body. Thus, the PEG polymers in PEGylated nanoparticle with rigid water core could freely diffuse on the surface. However, because of the rigid water core, the lipid bilayer on the surface could barely deform. All other conditions are the same as the ones in Fig. 2B of main text. As given in Fig. S6, the whole membrane wrapping process is similar as the one of PEGylated liposome. The PEG polymers aggregate in the contact region due their mobility. The half-wrapped PEGylated nanoparticle with rigid water core bounces back to the less wrapped state afterwards. Both the detailed information about wrapping ratio and ligand-receptor binding ratio are identical as that of PEGylated liposome (Fig. S6.B and C). However, the asphericity value of rigid NP is kept constant. Thus we could confirm that the PEG mobility is the main reason for the PEG polymers aggregation and 'bouncing back' of PEGylated liposome.

References

[1] P. J. Hoogerbrugge and J. M. V. A. Koelman. Simulating microscopic hydrodynamic phenomena with dissipative particle dynamics. *Europhys. Lett.*, 19(3):155, 1992.

[2] Robert D Groot and Patrick B Warren. Dissipative particle dynamics: Bridging the gap between atomistic and mesoscopic simulation. *J. Chem. Phys.*, 107(11):4423, 1997.

[3] Isaac Salib, Xin Yong, Emily J Crabb, Nicholas M Moellers, Gerald T McFarlin I. V., Olga Kuksenok, and Anna C Balazs. Harnessing fluid-driven vesicles to pick up and drop off janus particles. *ACS Nano*, 7(2):1224–1238, 2013.

[4] A Gama Goicochea, E Mayoral, J Klapp, and C Pastorino. Nanotribology of biopolymer brushes in aqueous solution using dissipative particle dynamics simulations: an application to peg covered liposomes in a theta solvent. *Soft Matter*, 10(1):166–174, 2014.

[5] Dmitry A Fedosov, George Em Karniadakis, and Bruce Caswell. Steady shear rheometry of dissipative particle dynamics models of polymer fluids in reverse poiseuille flow. *J. Chem. Phys*, 132(14):144103, 2010.

[6] Xin Yong, Emily J Crabb, Nicholas M Moellers, and Anna C Balazs. Self-healing vesicles deposit lipid-coated janus particles into nanoscopic trenches. *Langmuir*, 29(52):16066–16074, 2013.

[7] Zhiqiang Shen, Mu-Ping Nieh, and Ying Li. Decorating nanoparticle surface for targeted drug delivery: opportunities and challenges. *Polymers*, 8(3):83, 2016.

[8] Hong-Ming Ding and Yu-Qiang Ma. Theoretical and computational investigations of nanoparticle–biomembrane interactions in cellular delivery. *Small*, 11(9-10):1055–1071, 2015.

[9] Ying Li, Wylie Stroberg, Tae-Rin Lee, Han Sung Kim, Han Man, Dean Ho, Paolo Decuzzi, and Wing Kam Liu. Multiscale modeling and uncertainty quantification in nanoparticle-mediated drug/gene delivery. *Comput. Mech.*, 53(3):511–537, 2014.

[10] Ying Li, Martin Kröger, and Wing Kam Liu. Endocytosis of pegylated nanoparticles accompanied by structural and free energy changes of the grafted polyethylene glycol. *Biomaterials*, 35(30):8467–8478, 2014.

[11] Liuyang Zhang and Xianqiao Wang. Nanotube-enabled vesicle–vesicle communication: A computational model. *J. Phys. Chem. Lett.*, 6(13):2530–2537, 2015.

[12] Liuyang Zhang and Xianqiao Wang. Coarse-grained modeling of vesicle responses to active rotational nanoparticles. *Nanoscale*, 7(32):13458–13467, 2015.

[13] Jinglei Hu, Reinhard Lipowsky, and Thomas R Weikl. Binding constants of membrane-anchored receptors and ligands depend strongly on the nanoscale roughness of membranes. *Proc. Natl. Acad. Sci. USA*, 110(38):15283–15288, 2013.

[14] Andrea Grafmüller, Julian Shillcock, and Reinhard Lipowsky. Pathway of membrane fusion with two tension-dependent energy barriers. *Phys. Rev. Lett.*, 98(21):218101, 2007.

[15] Andrea Grafmüller, Julian Shillcock, and Reinhard Lipowsky. The fusion of membranes and vesicles: pathway and energy barriers from dissipative particle dynamics. *Biophys. J.*, 96(7):2658–2675, 2009.

[16] Robert D Groot and KL Rabone. Mesoscopic simulation of cell membrane damage, morphology change and rupture by nonionic surfactants. *Biophys. J.*, 81(2):725–736, 2001.

[17] Maddalena Venturoli, Maria Maddalena Sperotto, Marieke Kranenburg, and Berend Smit. Mesoscopic models of biological membranes. *Phys. Rep.*, 437(1):1–54, 2006.

[18] M Mutz and W Helfrich. Bending rigidities of some biological model membranes as obtained from the fourier analysis of contour sections. *J. Phys.*, 51(10):991–1001, 1990.

[19] Rüdiger Goetz, Gerhard Gompper, and Reinhard Lipowsky. Mobility and elasticity of self-assembled membranes. *Phys. Rev. Lett.*, 82(1):221, 1999.

[20] Ying Li, Martin Kröger, and Wing Kam Liu. Shape effect in cellular uptake of pegylated nanoparticles: comparison between sphere, rod, cube and disk. *Nanoscale*, 7(40):16631–16646, 2015.

[21] Eun Chul Cho, Leslie Au, Qiang Zhang, and Younan Xia. The effects of size, shape, and surface functional group of gold nanostructures on their adsorption and internalization by cells. *Small*, 6(4):517–522, 2010.

[22] Carl D Walkey, Jonathan B Olsen, Hongbo Guo, Andrew Emili, and Warren C. W. Chan. Nanoparticle size and surface chemistry determine serum protein adsorption and macrophage uptake. *J. Am. Chem. Soc.*, 134(4):2139–2147, 2012.

[23] Adam de la Zerda, Sunil Bodapati, Robert Teed, Salomon Y May, Scott M Tabakman, Zhuang Liu, Butrus T Khuri-Yakub, Xiaoyuan Chen, Hongjie Dai, and Sanjiv S Gambhir. Family of enhanced photoacoustic imaging agents for high-sensitivity and multiplexing studies in living mice. *ACS Nano*, 6(6):4694–4701, 2012.

[24] Yegor A Domanov, Sophie Aimon, Gilman ES Toombes, Marianne Renner, François Quemeneur, Antoine Triller, Matthew S Turner, and Patricia Bassereau. Mobility in geometrically confined membranes. *Proceedings of the National Academy of Sciences*, 108(31):12605–12610, 2011.

[25] H Jelger Risselada and Siewert J Marrink. Curvature effects on lipid packing and dynamics in liposomes revealed by coarse grained molecular dynamics simulations. *Physical Chemistry Chemical Physics*, 11(12):2056–2067, 2009.

[26] Norbert Kučerka, Yufeng Liu, Nanjun Chu, Horia I Petrache, Stephanie Tristram-Nagle, and John F Nagle. Structure of fully hydrated fluid phase dmpc and dlpc lipid bilayers using x-ray scattering from oriented multilamellar arrays and from unilamellar vesicles. *Biophys. J.*, 88(4):2626–2637, 2005.

[27] Greger Orädd, Göran Lindblom, and Philip W Westerman. Lateral diffusion of cholesterol and dimyristoylphosphatidylcholine in a lipid bilayer measured by pulsed field gradient nmr spectroscopy. *Biophys. J.*, 83(5):2702–2704, 2002.

[28] Steve Plimpton. Fast parallel algorithms for short-range molecular dynamics. *J. Comput. Phys.*, 117(1):1–19, 1995.

[29] Bingbing Hong, Feng Qiu, Hongdong Zhang, and Yuliang Yang. Budding dynamics of individual domains in multicomponent membranes simulated by n-varied dissipative particle dynamics. *J. Phys. Chem. B*, 111(21):5837–5849, 2007.

[30] Hong-ming Ding and Yu-qiang Ma. Computer simulation of the role of protein corona in cellular delivery of nanoparticles. *Biomaterials*, 35(30):8703–8710, 2014.

[31] Ye Li, Xianren Zhang, and Dapeng Cao. Nanoparticle hardness controls the internalization pathway for drug delivery. *Nanoscale*, 7(6):2758–2769, 2015.

[32] Huajian Gao, Wendong Shi, and Lambert B Freund. Mechanics of receptor-mediated endocytosis. *Proc. Natl. Acad. Sci. USA*, 102(27):9469–9474, 2005.

[33] JMHM Scheutjens and GJ Fleer. Statistical theory of the adsorption of interacting chain molecules. 1. partition function, segment density distribution, and adsorption isotherms. *J. Phys. Chem.*, 83(12):1619–1635, 1979.

[34] CM Wijmans and Ekaterina B Zhulina. Polymer brushes at curved surfaces. *Macromolecules*, 26(26):7214–7224, 1993.

[35] Wolfgang Helfrich. Elastic properties of lipid bilayers: theory and possible experiments. *Ze. Naturforsch. C*, 28(11-12):693–703, 1973.

[36] WT Góźdź. Deformations of lipid vesicles induced by attached spherical particles. *Langmuir*, 23(10):5665–5669, 2007.

[37] Jiuling Wang, Haimin Yao, and Xinghua Shi. Cooperative entry of nanoparticles into the cell. *J. Mech. Phys. Solids*, 73:151–165, 2014.

[38] Markus Deserno. Elastic deformation of a fluid membrane upon colloid binding. *Phys. Rev. E*, 69(3):031903, 2004.

[39] James Kennedy. Particle swarm optimization. In *Encyclopedia of machine learning*, pages 760–766. Springer, 2011.